広島大学学位請求論文

Phase Behavior of Aqueous Solution of Poly(ethylene oxide)–Poly(propylene oxide) Alternating Multiblock Copolymer

（ポリエチレンオキシド-ポリプロピレンオキシド交互マルチブロックコポリマー水溶液の相挙動）

2020 年

広島大学大学院理学研究科

化学専攻

堀内　輔

目 次

1. 主論文

Phase Behavior of Aqueous Solution of Poly(ethylene oxide)–Poly(propylene oxide) Alternating Multiblock Copolymer

（ポリエチレンオキシド‐ポリプロピレンオキシド交互マルチブロックコポリマー水溶液の相挙動）

堀内　輔

2. 公表論文

(1) Horiuchi, Tasuku; Sakai, Takamasa; Sanada, Yusuke; Watanabe, Keisuke; Aida, Misako; Katsumoto, Yukiteru

Association Behavior of Poly(ethylene oxide)–Poly(propylene oxide) Alternating Multiblock Copolymers in Water toward Thermally Induced Phase Separation.

Langmuir **2017**, *33*, 14649–14656.

(2) Horiuchi, Tasuku; Rikiyama, Kazuaki; Sakanaya, Kenji; Sanada, Yusuke; Watanabe, Keisuke; Aida, Misako; Katsumoto, Yukiteru

Effect of Molecular Weight on Cloud Point of Aqueous Solution of Poly(ethylene oxide)–Poly(propylene oxide) Alternating Multiblock Copolymer.

J. Oleo Sci. (in press)

3. 参考論文

(1) Rikiyama, Kazuaki; Horiuchi, Tasuku; Koga, Naoyuki; Sanada, Yusuke; Watanabe, Keisuke; Aida, Misako; Katsumoto, Yukiteru

Micellization of Poly(Ethylene Oxide)–Poly(Propylene Oxide) Alternating Multiblock Copolymers in Water.

Polymer **2018**, *156*, 102–110.

主論文

Phase Behavior of Aqueous Solution of Poly(ethylene oxide)–Poly(propylene oxide) Alternating Multiblock Copolymer

Tasuku Horiuchi

Department of Chemistry, Graduate School of Science,
Hiroshima University

Acknowledgements

This thesis would not have been completed without the support of others. First, I would like to gratefully acknowledge Professor Misako Aida for valuable guidance, suggestion, and encouragement as my supervisor. I would also like to acknowledge Professor Kazumasa Okada and Dr. Dai Akase for them suggestion and encouragement. I am deeply grateful to Professor Taka-aki Ishibashi at the University of Tsukuba for helpful guidance and encouragement as my tutor when he has belonged to Hiroshima University. I would like to acknowledge Professor Katsuyoshi Yamasaki and Professor Ken-ichi Saitow for vigorous discussion and valuable comments as my thesis committee. I would also like to acknowledge all the members of department of chemistry at Hiroshima University.

I would like to gratefully acknowledge Professor Yukiteru Katsumoto for various discussion, guidance, suggestion, and continuous encouragement over the years. He gave me many significant things for my way of living. I would like to acknowledge Professor Keishi Negita, Dr. Yusuke Sanada, and Dr. Keisuke Watanabe for helpful advice, discussion, and encouragement. I would also like to acknowledge all the members of department of chemistry at Fukuoka University.

I would like to acknowledge Professor Takamasa Sakai at the University of Tokyo for giving us material samples and advice in regards to synthesis of polymers.

I would like to thank Mr. Kazuaki Rikiyama for valuable discussion and spending common times for a long time as my teammates. I would also like to thank all the member of the quantum chemistry research group at Hiroshima University and all the member of the physical chemistry research group at Fukuoka University.

Finally, I would like to thank my family, friends, and all other people who have given me their help, advice, and kindness.

Contents

CHAPTER 1

General Introduction

Thermoresponsive polymers are a class of smart materials. Those properties are significantly changed in a control fashion by external stimuli. To develop proteins mimics by using synthetic polymers is a great challenge for the polymer scientists. The block design of copolymers is an effective strategy to prepare protein mimics by using synthetic polymers. An alternative way is to control precisely the monomer sequence in the polymer chain that corresponds to the primary structure of proteins. However, the interaction among the monomers incorporated in the chain often makes it difficult to predict the macroscopic properties of the final products. In comparison with the monomer sequence control, the block design has advantages on the prediction of physicochemical properties of the resultant copolymer and also on the scale-up of the production processes. A block is expected to retain the characteristics as the homopolymer. Therefore, well-characterized homopolymers can be used as a block library.

Amphiphilic block copolymers of poly(ethylene oxide) (PEO) and poly(propylene oxide) (PPO), PEO–PPO block copolymers have also been considered as smart materials, because the morphology of aggregates change responding to an external stimulus. The common stimulus used are temperature variations. For example, the aqueous solutions of PEO–PPO block copolymers have the critical micelle temperature. Moreover, some of them show a sol–gel transition upon heating, which is attractive for the design of injectable matrices for minimally invasive biomedical applications. Although the PEO–PPO alternating multiblock (AMB) copolymers possess interesting features as above mentioned, the fundamental aspects have yet to be fully revealed. In this study, we have studied the phase behavior of the aqueous solution of PEO–PPO AMB copolymers by the use of the transmittance measurement and the light scattering technique.

CHAPTER 2

Characteristics of PEO–PPO AMB Copolymer

2.1 Introduction

Block copolymers of poly(ethylene oxide) (PEO) and poly(propylene oxide) (PPO) have received much attention for many decades because of their potential as nonionic macromolecular surfactants, which can yield ordered structures with various morphologies, such as micelles, lamellae, and vesicles. Their ability to greatly enhance the solubility of hydrophobic solutes in solutions has many important industrial and biomedical applications[1]. Many types of configurations for the block copolymers have been examined for micellar solubilization: linear PEO–PPO diblock[2], linear and bifunctional PEO–PPO–PEO triblock (Pluronic or poloxamer)[3], branched four-arm PEO–PPO counterpart block (Tetronic)[2], and so on. Use of these block copolymers as vehicles for the administration of drugs is one of the most desirable outcomes.

The PEO–PPO block copolymers have also been considered as smart materials because the morphology of aggregates may change by responding to an external stimulus. The common stimuli used are temperature variations. For example, the aqueous solutions of many kinds of PEO–PPO block copolymers have the critical micelle temperature[4]. Moreover, some of them show a sol–gel transition upon heating, which is attractive to the design of injectable matrices for minimally invasive biomedical applications[5].

The block configuration of the copolymers substantially modifies their solution properties. Nagarajan and Ganesh have theoretically studied the solubilization of hydrocarbons in micelles formed by PEO–PPO block copolymers with the same PPO–PEO composition but a different block configuration[6–8]. They predict that the diblock $EO_{200}PO_{64}$ copolymer can dissolve hydrocarbons in the hydrophobic core of micelles much more than the triblock $EO_{100}PO_{64}EO_{100}$ copolymer, where EO is the ethylene oxide ($-CH_2-CH_2-O-$) unit, PO is the propylene oxide ($-CH(CH_3)-CH_2-O-$) unit, and the subscripts represent the number of repeating units in each block[7]. The diblock $EO_{100}PO_{32}$ copolymer may form a micelle that keeps hydrocarbons solubilized as much as the $EO_{100}PO_{64}EO_{100}$

copolymer, but the aggregation number of the diblock copolymers per micelle should become twice that of the triblock one.

Pluronics (poloxamers) are commercially available PEO–PPO–PEO triblock copolymers having a linear symmetric configuration. Solution properties of Pluronics have been investigated systematically[3] because the polymer samples with various copolymer composition ratios and molecular weights are commercially available. The aqueous solution of Pluronics shows the unimer–micelle transition. At a low temperature or concentration, the triblock copolymer exists as a unimer in the aqueous solution, but thermodynamically stable micelles are formed with increasing temperature or concentration. This process has been investigated by using surface tension[9], light scattering[10], and dye solubilization[11].

In contrast to the PEO–PPO–PEO triblock copolymers, PEO–PPO alternating multiblock (AMB) copolymers have been less investigated. For the aqueous solution of PEO–PPO copolymers, Sosnik and Cohn have reported that the viscosity after the thermal gelation drastically increases when the configuration is changed from triblock to AMB[12]. Sun et al. have revealed that the aqueous solution of Pluronics often shows the re-entrant sol–gel–sol transition (the system changes from sol to gel to sol with increasing temperature), whereas that of the PEO–PPO AMB copolymer undergoes only the sol–gel transition in the same temperature range[13]. Both of the groups have suggested that the size of aggregates generated by the PEO–PPO AMB copolymers is markedly larger than that of Pluronics when the molecular weights of the PEO and PPO blocks are similar.

Although there are some reports that focus on the thermal gelation of the aqueous solution of PEO–PPO AMB copolymers, much less effort has been spent on understanding the association behavior of copolymers in water, which is important as a fundamental step of the thermal gelation. In this paper, we have studied the phase behavior of the aqueous solution of PEO–PPO AMB copolymers by the use of the transmittance measurement and the light scattering technique.

2.2 Experimental Section

2.2.1 Preparation of PEO–PPO AMB Copolymers

α,ω-Diamino PPO (JEFFAMINE D-2000, weight-average molecular weight (M_w) = 2000) was kindly supplied by Huntsman Corporation. α,ω-Disuccinimidyl PEOs (SUNBRIGHT DE-100HS and DE-034HS, M_w = 10 000 and 3400, respectively) were purchased from NOF Corporation. Chloroform was obtained from Wako Pure Chemical Industries. All reagents were used as received. The PEO–PPO AMB copolymer was prepared by a dehydrated condensation reaction (Scheme 1). α,ω-Disuccinimidyl PEO and α,ω-diamino PPO were individually dissolved into chloroform at 0 °C. The solutions of the prepolymer were mixed, followed by gently stirring overnight. The resultant solution was dialyzed against methanol for 1 day and then against distilled water for 2 days. The product was obtained as a white solid by freeze-drying.

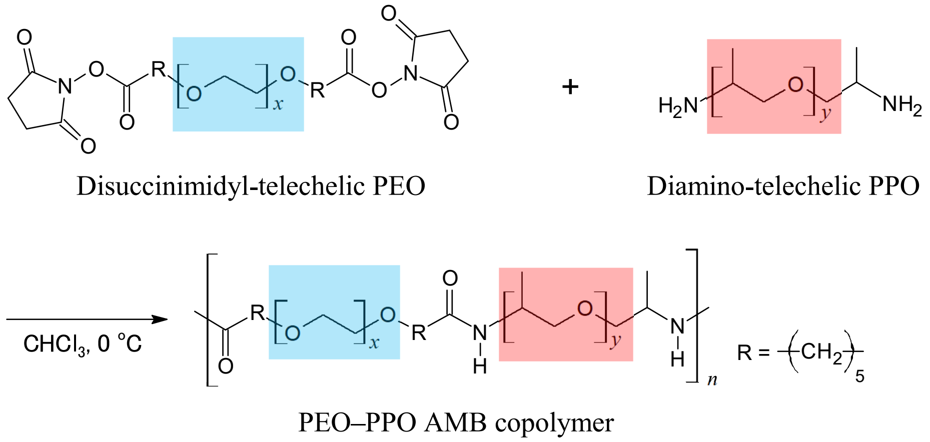

Scheme 1. Preparation of a PEO-PPO AMB copolymer.

2.2.2 Size Exclusion Chromatography

M_w, the number-average molecular weight (M_n), and the polydispersity (M_w/M_n) were determined by size exclusion chromatography (SEC). SEC consists of a Jasco Intelligent HPLC system equipped with a guard column (SB-G, Shodex), two separation columns (SB-802.5HQ and SB-806MHQ, Shodex), and a refractive index detector (RI-2031Plus, Jasco). *N*,*N*-Dimethylformamide (HPLC-grade, Wako) with 10 mM LiBr was used as an eluent. The flow rate was 0.35 mL min^{-1} at 60 °C. The SEC chromatogram was calibrated with a series of standard polystyrene samples with 10 different peak-top molecular weights (M_p) from 1.22×10^3 to 2.70×10^6 (Standard SM-105, Shodex).

2.2.3 ^{1}H NMR and IR Spectroscopies

^{1}H NMR spectra were recorded with an Ascend 400 (Bruker) at 400 MHz to determine the ratio of EO units to PO units (*EO/PO*) in the PEO–PPO AMB copolymers. *EO/PO* was evaluated by comparing the peak area of the methylene protons in the EO unit ($\delta \approx 3.7$ ppm) with that of the methyl protons in the PO unit ($\delta \approx 1.2$ ppm). All spectra were obtained at room temperature with 0.5 wt % D_2O solutions. IR spectra were measured with a resolution of 2 cm^{-1} by a coaddition of 128 scans using a Nicolet 6700 FTIR spectrometer equipped with a DTGS detector. Thin films of the samples were prepared by spin-coating on a KBr plate from an acetone solution.

2.2.4 Turbidity Measurements

The temperature dependence of the transmittance of the polymer solution was monitored using a UV–vis spectrophotometer (V-630iRM, Jasco) equipped with a temperature controller (ETCS-761, Jasco). The heating rate was 0.1 °C min^{-1}. The cloud point T_c was defined as the temperature at which the first derivative of the transmittance curve becomes minimum.

2.2.5 Dynamic Light Scattering Measurements

Dynamic light scattering (DLS) measurements were carried out using a Zetasizer Nano S (Malvern). A 4 mW He–Ne laser (wavelength $\lambda = 632.8$ nm) was used as the incident light, and the scattering angle was 173°. Large particle contaminants were removed by a filter membrane with 0.20 μm of pore size.

2.2.6 Static Light Scattering Measurements

Static light scattering (SLS) measurements were carried out to determine M_w and the second virial coefficient A_2 under the same experimental setup for DLS measurements. The scattering intensity was integrated for 10 s, and the average of ca. 50 samplings was calculated. The SLS data were analyzed by means of Debye plot with the following equation:

$$\frac{Kc}{R_\theta} = \frac{1}{M_w} + 2A_2c \quad (1)$$

where K is the optical constant, c is the polymer concentration, and R_θ is the excess Rayleigh ratio[14]. K equals $4\pi^2 n_0^2(\mathrm{d}n/\mathrm{d}c)^2/N_A\lambda^4$, where n_0 is the refractive index of water, $\mathrm{d}n/\mathrm{d}c$ is the refractive index increment of the sample solution, λ is the wavelength of the incident light, and N_A is the Avogadro constant. The reflective index was measured by the use of a refractometer (RX-5000i, Atago) under temperature-controlled conditions.

2.3 Results and Discussion

2.3.1 Characterization of PEO–PPO AMB Copolymers and Phase Behavior of Aqueous Solution

Figure 2-1 shows the SEC chart for the PEO and PPO prepolymers and the products. Because the M_w values of the products are much larger than those of the prepolymers, it can be presumed that PEO–PPO AMB copolymers are generated. The formation of the amide groups has been confirmed by IR spectroscopy (the result is shown in Figure 2-2). The M_w and M_w/M_n values of the PEO–PPO AMB copolymers and the prepolymers estimated by SEC are summarized in Table 1. Note that the M_w values of the PEO and PPO prepolymers determined by SEC are over- or underestimated compared with those found in the catalog provided by the reagent suppliers. By reference to M_w of the PEO–PPO AMB copolymers (1.74×10^5 and 5.7×10^4 g mol^{-1}), the number of PEO–PPO repeating pairs in the copolymer is estimated to be about 8–9. For $(EO_{220}PO_{33})_8$, *EO/PO* from the values in the supplier's catalog is 6.7/1.0, whereas that estimated by ^{1}H NMR spectroscopy is 7.2/1.0. *EO/PO* of $(EO_{68}PO_{33})_9$ shows a similar tendency; that is, the EO content of the AMB copolymers is slightly larger than that in preparation. These results suggest that the PEO–PPO AMB copolymers are successfully obtained. The number of PEO–PPO repeating pairs of the copolymer is larger than that

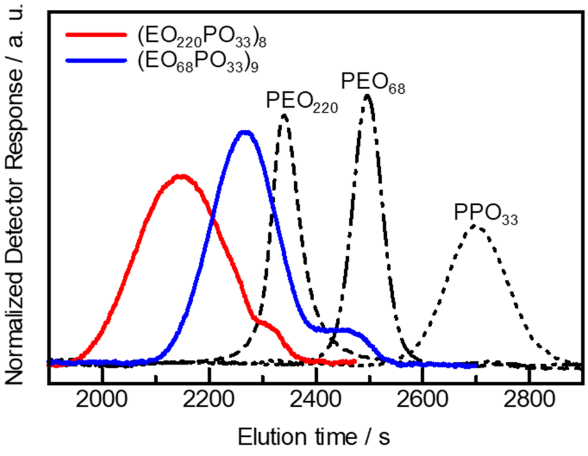

Figure 2-1. SEC chart of α,ω-diamino PPO, α,ω-disuccinimidyl PEO, and the PEO–PPO AMB copolymers $(EO_{220}PO_{33})_8$ and $(EO_{68}PO_{33})_9$.

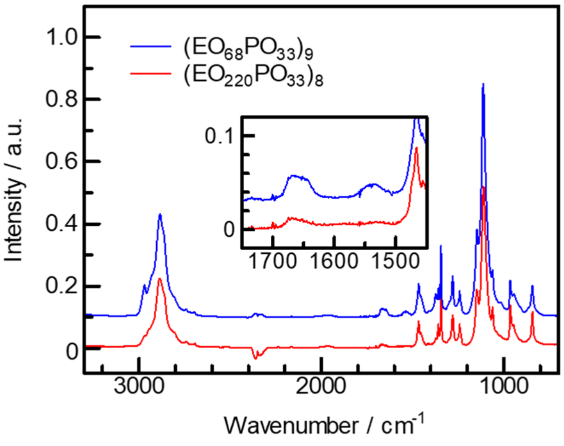

Figure 2-2. IR spectra of the PEO–PPO AMB copolymers. Thin films of the samples was prepared by spin-coating on a KBr plate from the acetone solution. The amide I and II bands appear at ~1670 and ~1540 cm^{-1}, respectively.

of the PEO–PPO AMB copolymers ever reported. The number of PEO–PPO repeating pairs for the PEO–PPO AMB copolymer reported by Sosnik and Cohn is about 3[12], and that reported by Sun et al. is about 4[13].

Because PEO is hydrophilic and PPO is hydrophobic, the PEO–PPO AMB copolymers are expected to act as a nonionic amphiphilic polymer in water. Figure 2-3 shows the transmittance curves for the 2.0 wt % aqueous solution of the PEO–PPO AMB copolymers measured with light at 650 and 350 nm. For $(EO_{220}PO_{33})_8$, the transmittance of the 650 nm light drastically decreases at around 60 °C,

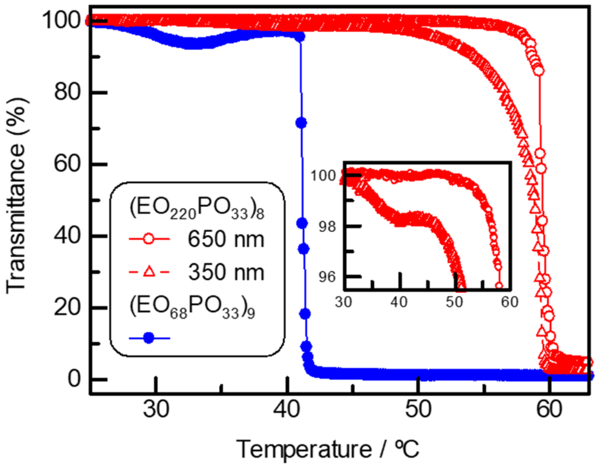

Figure 2-3. Transmittance curves of the PEO–PPO AMB copolymer $(EO_{220}PO_{33})_8$ and $(EO_{68}PO_{33})_9$ at the 2.0 wt% aqueous solution measured with light at 650 and 350 nm.

Table 1. Molecular weight (M_w) and polydispersity (M_w/M_n) of PEO, PPO prepolymers, and PEO–PPO AMB copolymers.

	supplier's[a]			measured M_w (M_w/M_n)			
sample	M_w	x	y	SEC[b]	SLS[c]	EO/PO[d]	f_{PEO}[e]
EO_{220}	1.0×10^4	220	—	2.0×10^4 (1.2)	—	—	—
EO_{68}	3.4×10^3	68	—	5.0×10^3 (1.0)	—	—	—
PO_{33}	2.0×10^3	—	33	1.4×10^3 (1.0)	—	—	—
$(EO_{220}PO_{33})_8$	—	220	33	1.7×10^5 (2.1)	1.3×10^5	7.2/1.0	0.83
$(EO_{68}PO_{33})_9$	—	68	33	5.7×10^4 (2.0)	4.1×10^4	2.5/1.0	0.55

[a] Values given by the catalog of the supplier. [b] SEC with polystyrene standards. [c] SLS with the Debye plot. [d] Estimated by ^1H NMR. [e] f_{PEO}, calculated by using the values in the supplier's catalog.

which corresponds to the cloud point (T_c). Although the slope of the transmittance curve of the 350 nm light is less steep than that of the 650 nm light, the T_c value does not significantly depend upon the wavelength of the light (59.7 °C for T_c determined by the 650 nm light and 59.3 °C by the 350 nm light). By closely inspecting the transmittance curve of the 350 nm light shown in Figure 2-3, one can see a small stepwise decrement of the transmittance at around 40 °C. For $(EO_{68}PO_{33})_9$, a precursory drop of the transmittance becomes more significant; the transmittance of the 650 nm light has a minimum at around 34 °C, followed by recovering in the range of 38–41 °C, and then shows a large decrement to 0 at around 42 °C. T_c of the aqueous solution of $(EO_{68}PO_{33})_9$ is estimated from this large decrement of the transmittance.

The microscopic image of the aqueous PEO–PPO AMB copolymer solution obtained above T_c shows dropletlike patterns, as shown in Figure 2-4. Linse has theoretically indicated that an aqueous Pluronic solution undergoes phase separation upon heating[4]. Thus, we have presumed that T_c observed here is associated with the phase separation of the aqueous solution of the PEO–PPO AMB copolymers. The concentration dependence of T_c gives a rough estimation of the phase boundary curve of the system. Figure 2-5 demonstrates that the aqueous solution of the PEO–PPO AMB copolymer has a lower critical solution temperature (LCST)-type phase diagram. The concentration dependence

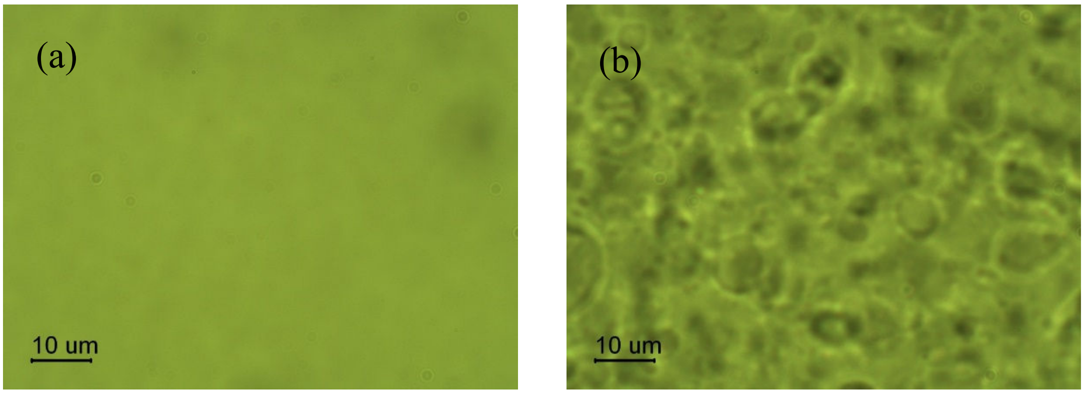

Figure 2-4. Optical micrographs of the 2.0 wt% aqueous solution of the PEO–PPO AMB copolymer $(EO_{220}PO_{33})_8$ at (a) ~25 °C and (b) ~70 °C. The edge of the coverslip was sealed with an epoxy glue.

of the transmittance curve of the 650 nm light is shown in Figure 2-6. T_c becomes almost independent from the concentration above 0.4 wt %. For $(EO_{220}PO_{33})_8$, the phase boundary curve seems to have a shallow minimum at around 0.3 wt % and 58 °C, which should correspond to the LCST. On the other hand, the LCST for $(EO_{68}PO_{33})_9$ is around 42 °C. Note that the critical solution concentration for $(EO_{68}PO_{33})_9$ is difficult to be identified because the concentration dependence at > 0.5 wt % is very small.

It has been known that the aqueous solution of PEO homopolymers undergoes LCST-type phase separation[15]. Thus, it is possible that the lowering solubility of the PEO–PPO AMB copolymer in water with an elevating temperature is partially attributed to the instability of PEO chains in hot water[16]. Indeed, the hydration number of the ethylene oxide unit, which is 4 below 30 °C, gradually decreases to 2 at 70 °C irrespective of M_w[17]. However, the PEO chain at 58 °C may not be hydrophobic enough to make the PEO–PPO AMB copolymer unstable because the phase separation of PEO homopolymers in water occurs over 100 °C[15]. It is worth noting that the theta temperature (T_θ) of the PEO/water system is around 96 °C[18], indicating that a repulsive interaction among the PEO chains in water is still predominant at 58 °C. It is inferred, therefore, that the driving force of the

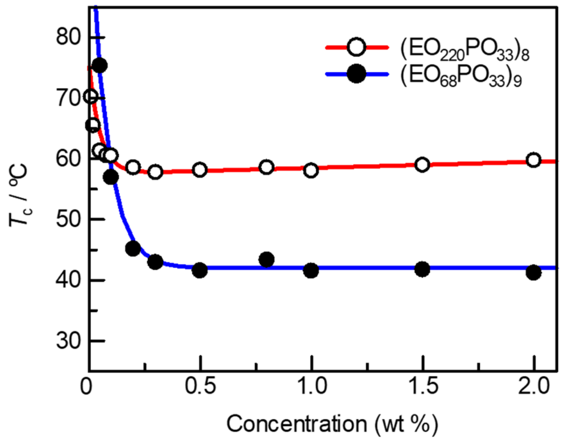

Figure 2-5. Concentration dependence of T_c for the aqueous solutions of $(EO_{220}PO_{33})_8$ and $(EO_{68}PO_{33})_9$. T_c is determined by the transmittance curve with light at 650 nm.

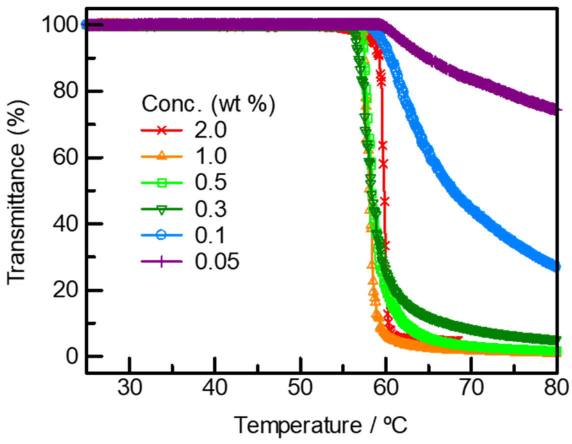

Figure 2-6. Transmittance curves of the aqueous solution of the PEO–PPO AMB copolymer $(EO_{220}PO_{33})_8$ at various concentrations measured with light at 650 nm for the heating process.

phase separation of the aqueous PEO–PPO AMB solution is mainly due to the hydrophobic interaction between the PPO blocks similar to that for Pluronics[11]. The phase boundary curve for the aqueous solution of $(EO_{68}PO_{33})_9$ shifts down compared with that of $(EO_{220}PO_{33})_8$, indicating that the increment of the weight fraction of PPO lowers the stability of the copolymer in water. This will be discussed again in the later section.

For the nonionic amphiphilic compounds, it is generally considered that the hydrophilic–lipophilic balance is the primary factor to estimate T_c of the aqueous solutions[19, 20]. The weight fraction of PEO in the copolymers, f_{PEO}, of $(EO_{220}PO_{33})_8$ is 0.83, whereas that of Pluronic F88 $(EO_{100}PO_{39}EO_{100})$ is 0.80. The f_{PEO} values of $(EO_{68}PO_{33})_9$ and Pluronic P85 $(EO_{25}PO_{39}EO_{25})$ are 0.55 and 0.50, respectively. In this context, therefore, the hydrophilicities of $(EO_{220}PO_{33})_8$ and Pluronic F88 should be similar. This may be the same for $(EO_{68}PO_{33})_9$ and Pluronic P85. However, the T_c values of the 1 wt % aqueous solutions of Pluronic P85 and F88 are much higher than those of the corresponding PEO–PPO AMB copolymers (T_c for Pluronic P85 is 85 °C, and that for F88 is >100 °C)[3]. There are two possible factors to lower the stability of the PEO–PPO AMB copolymer in water compared with that of Pluronics. First, the PEO–PPO AMB copolymers prepared in this study contain two pentyl groups at the end of PEO blocks, which may make the copolymer more hydrophobic than Pluronic. Second, M_w of the PEO–PPO AMB copolymer is much larger than that of Pluronic, which may bring the LCST down similar to PEO homopolymers in water[15].

2.3.2 Thermally Induced Micellization of PEO–PPO AMB Copolymer

As mentioned in the previous section, the transmittance of the aqueous solution of the PEO–PPO AMB copolymers shows a precursory decrement at a temperature markedly lower than T_c. This implies that small aggregates are formed below T_c. When the aqueous solution of Pluronic is heated, micellization followed by phase separation has often been observed[3]. Figure 2-7 represents the temperature dependence of the scattering intensity of the 632.8 nm light at 173° scattering angle. For the 2.0 wt % aqueous solution of $(EO_{220}PO_{33})_8$, the scattering intensity starts increasing above 40 °C and tends to diverge toward T_c. The onset of the increment corresponds to the precursory decrement observed in the transmittance curve, indicating again that small aggregates are formed below T_c. A similar tendency is observed for the other concentration, as shown in Figure 2-8.

To estimate the size of the aggregates, DLS measurements have been carried out. Figure 2-9 shows the temperature change in the autocorrelation function, $g^{(1)}(\tau)$, for the 0.5 wt % aqueous solutions of the PEO–PPO AMB copolymers. Note that $g^{(1)}(\tau)$ cannot be obtained near T_c because the scattering intensity is too high. At 25 °C, there are two distinguishable relaxation modes for both

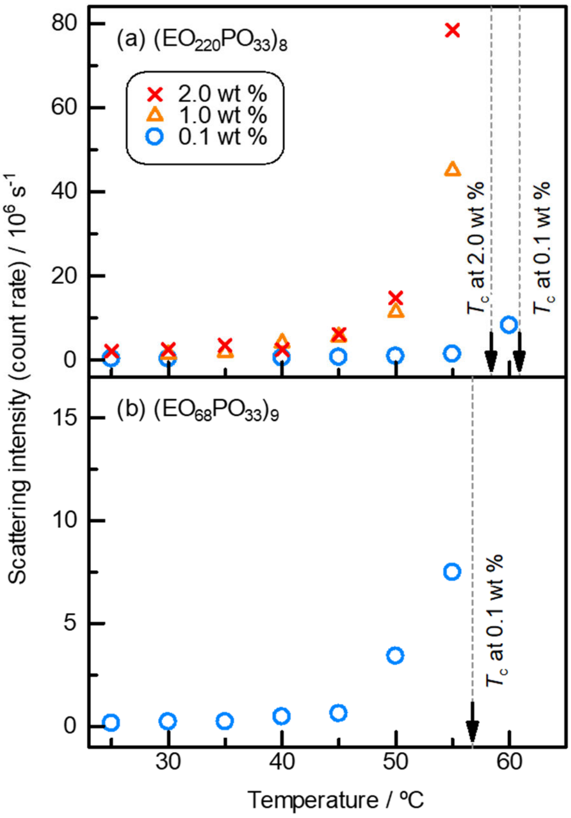

Figure 2-7. Temperature dependence of the scattering intensities (count rates) of the 632.8 nm light measured for the aqueous solutions of the PEO-PPO AMB copolymers (a) $(EO_{220}PO_{33})_8$ and (b) $(EO_{68}PO_{33})_9$. T_c indicated in the figure corresponds to that in Fig. 2-5.

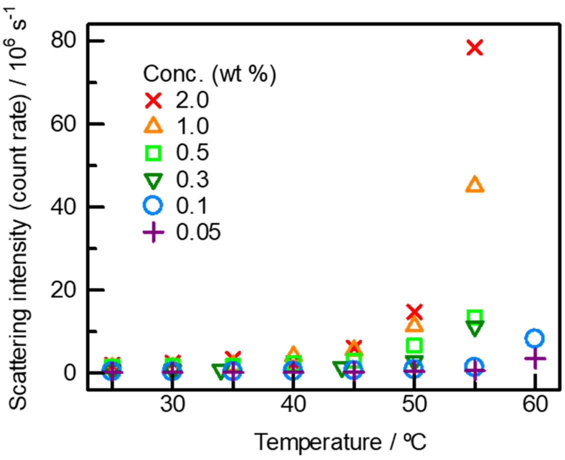

Figure 2-8. Temperature dependence of the scattering intensity of the 650 nm light measured for the aqueous solution of the PEO–PPO AMB copolymer $(EO_{220}PO_{33})_8$ at various concentrations during the heating process.

$(EO_{220}PO_{33})_8$ and $(EO_{68}PO_{33})_9$. On the other hand, $g^{(1)}(\tau)$ seems to become a single exponential as the temperature goes up. The Laplace inversion of $g^{(1)}(\tau)$ gives rise to a relaxation time distribution $A(\tau_R)$[21]. Figure 2-10 shows the temperature-dependent $A(\tau_R)$ for the aqueous solution of the PEO–PPO AMB copolymers. At 25 °C, $A(\tau_R)$ for both $(EO_{220}PO_{33})_8$ and $(EO_{68}PO_{33})_9$ are bimodal. The peaks are located at the relaxation times of τ_R = 30–50 and 400–850 μs. By use of the Stokes–Einstein equation with the viscosity of water at each temperature, the fast relaxation mode gives the hydrodynamic radii R_h = 10 nm for $(EO_{220}PO_{33})_8$ and R_h = 5 nm for $(EO_{68}PO_{33})_9$, which is possibly

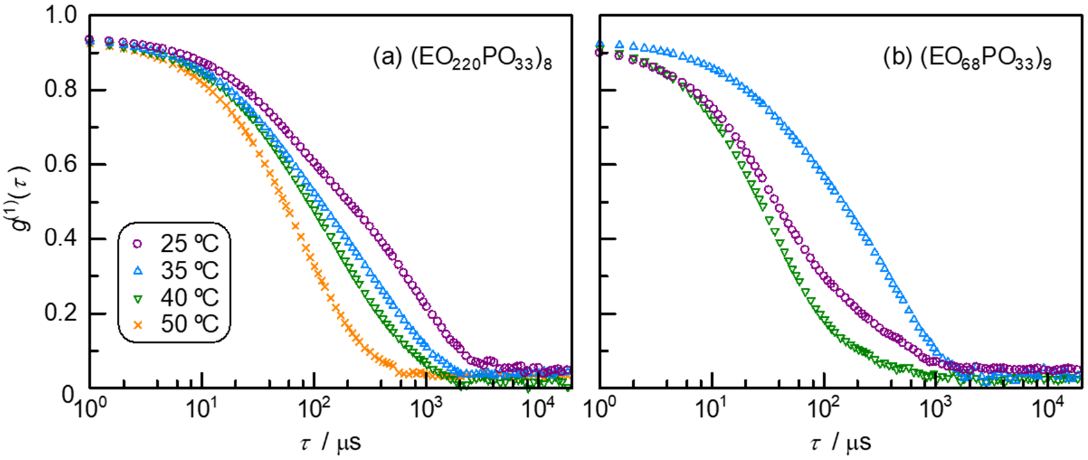

Figure 2-9. $g^{(1)}(\tau)$ for the aqueous solutions of the PEO–PPO AMB copolymer (a) $(EO_{220}PO_{33})_8$ and (b) $(EO_{68}PO_{33})_9$ at a concentration of 0.5 wt%.

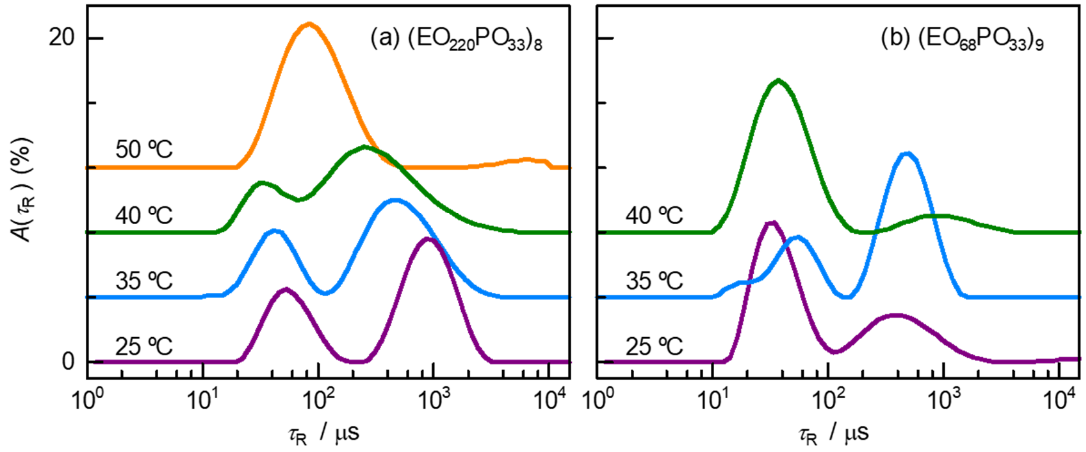

Figure 2-10. Temperature dependence of $A(\tau_R)$ for the aqueous solutions of the PEO–PPO AMB copolymer (a) $(EO_{220}PO_{33})_8$ and (b) $(EO_{68}PO_{33})_9$ at a concentration of 0.5 wt%.

due to the unimer of the PEO–PPO AMB copolymer. For PEO, R_h of a random coil chain with 1.0 × 10^5 g mol^{-1} is estimated to be around 10 nm.

Although the two relaxation modes cannot be directly converted to particle sizes in the solution[22], Figure 2-10 suggests that the PEO–PPO AMB copolymers are not homogeneously dispersed in the solution at 25 °C. The second relaxation mode possibly arises from the aggregate, whose R_h is roughly estimated to be 100–200 nm. It needs to be taken into consideration that the population of the aggregates should be very small, even though that of the second mode of $A(\tau_R)$ is relatively large. It has been considered that $A(\tau_R)$ is influenced by the scattering intensity which increases strongly with increasing particle size (see also Figure 2-11)[22]. Thus, the population of the unimer and aggregates is difficult to be estimated from the DLS results obtained here. We need further experiments for discussing the population of the unimer and aggregates, such as small-angle X-ray scattering and SLS with various scattering angles.

The aggregate is not a micelle because the fluorescence probe method does not support the

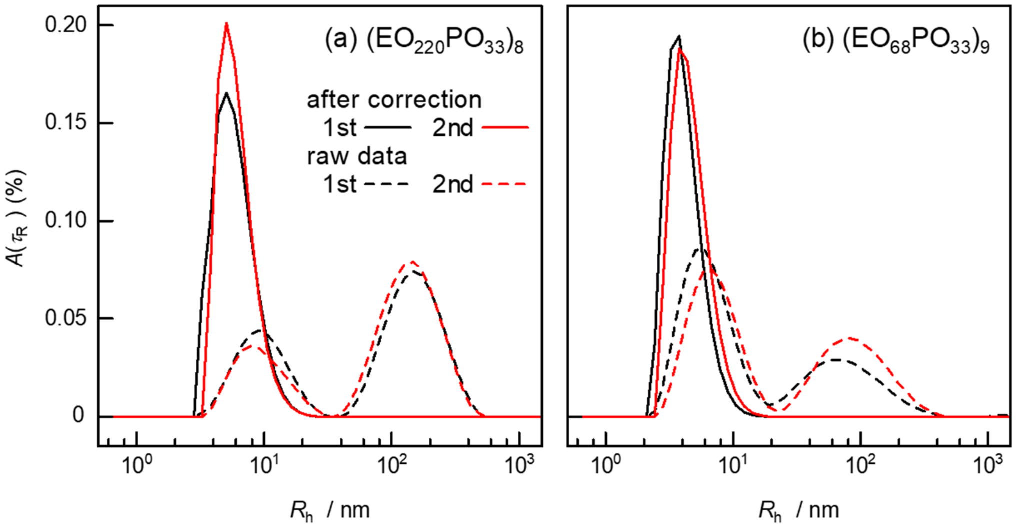

Figure 2-11. Apparent size-distribution for the PEO–PPO AMB copolymers in water, $A(R_h)$, at 25 °C and 0.5 wt%. The black and red colors indicate $A(R_h)$ measured under the same experimental condition, but the solutions are prepared individually. The dotted line shows the raw $A(R_h)$ derived from the Laplace inversion of the autocorrelation function, and the solid line represents $A(R_h)$ after the correction based upon the volume of the scattering particles (ref. 22 in the manuscript). It is very difficult to discuss the population of the unimer and aggregates by use of the DLS results.

existence of a hydrophobic core[20]. This kind of aggregates has also been found for relatively simple polymer solutions such as poly(*n*-hexyl isocyanate) in *n*-hexane and an atactic polystyrene in tetrahydrofuran[22]. The aggregates observed at a finite concentration in the solution have a diameter of a few hundred nanometers. Possible candidates for the binding force among the polymers are the van der Waals force, dipole–dipole interaction, solvent-mediated complexation, and so on. However, the origin of the force is still in dispute.

As the temperature increases, two modes in $A(\tau_R)$ for $(EO_{220}PO_{33})_8$ are fused and a unimodal peak at $\tau_R \approx 90$ μs appears at 50 °C. A similar result is obtained in the concentration range from 0.05 to 1.0 wt % (see Figure 2-12). This result suggests that a uniform-size aggregate with $R_h = 20$ nm is generated at around 50 °C. For $(EO_{68}PO_{33})_9$, the temperature dependence of $A(\tau_R)$ is a little more complicated. At 35 °C, the fast relaxation mode slightly shifts to a higher τ_R, and the peak of the slow mode becomes large. The further increase in temperature causes the growth of the peak for the fast relaxation mode again. At 40 °C, R_h estimated from the fast mode is 10 nm, which is slightly larger than R_h of the unimer of $(EO_{68}PO_{33})_9$.

It is likely that the aggregates with $R_h = 20$ nm for $(EO_{220}PO_{33})_8$ and those with $R_h = 10$ nm for $(EO_{68}PO_{33})_9$ are micelles of the PEO–PPO AMB copolymers. The micellization below T_c is commonly observed for the PEO–PPO–PEO triblock copolymer (Pluronic) in water[9–11, 23–26]. It has been known that several Pluronics in water form a micelle whose size is independent of temperature and concentration in a wide range. Pluronic L64 ($EO_{13}PO_{30}EO_{13}$) in water forms a micelle having a constant size over a wide concentration range[23]. For Pluronic P85 ($EO_{25}PO_{39}EO_{25}$) in water, the micelle size does not change from 15 to 50 °C[24]. Zhou and Chu have proposed that the balance between an increase in the aggregation number of the polymers and a dehydration of the polymer makes possible the micelle size to remain almost independent of temperature[10].

For Pluronic F88 ($EO_{100}PO_{39}EO_{100}$) in water, although multiple-size aggregates coexist at a low temperature, micelles appear with increasing temperature[25, 26]. Interestingly, the micelle size of Pluronic F88 (R_h = 10–20 nm) is similar to the size of the uniform-size aggregation of $(EO_{220}PO_{33})_8$ (R_h = 20 nm) observed at 50 °C. On the other hand, Brown et al. have revealed that R_h of the micelle of Pluronic P85 in water is around 8.0 nm, which is also similar to R_h of the aggregate of

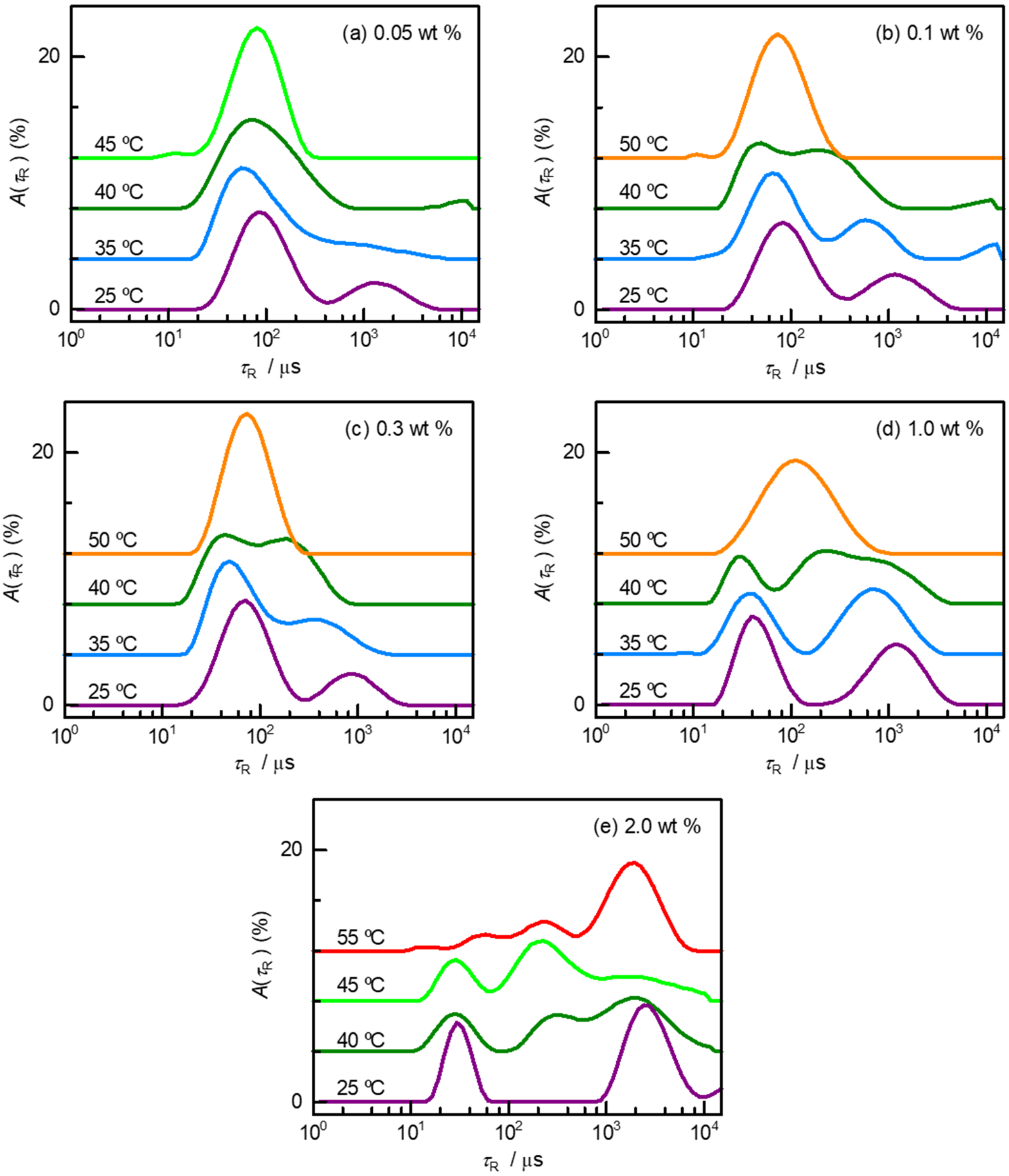

Figure 2-12. Temperature dependence of the relaxation time distributions $A(\tau_R)$ for the aqueous solution of the PEO–PPO AMB copolymer $(EO_{220}PO_{33})_8$ during heating process; (a) 0.05 wt %, (b) 0.1 wt %, (c) 0.3 wt %, (d) 1.0 wt %, (e) 2.0 wt %.

$(EO_{68}PO_{33})_9$[24]. These results imply that the micelle size of the PEO–PPO AMB copolymer is correlated with f_{PEO} similar to that for Pluronics.

A number of studies on Pluronics have pointed out that the micellization is caused by the hydrophobic interactions between the PO segments[11, 27, 28]. Differential scanning calorimetry measurements have shown an endothermic peak ($\Delta H > 0$) during the micellization[27], and the concentration dependence on the critical micelle temperature has also revealed that positive enthalpic change occurs[11]. Wanka *et al*. have pointed out that the ΔH at micellization is not correlated with the PEO block length but proportional to the PPO block length[27]. The hydrophobic interaction, which

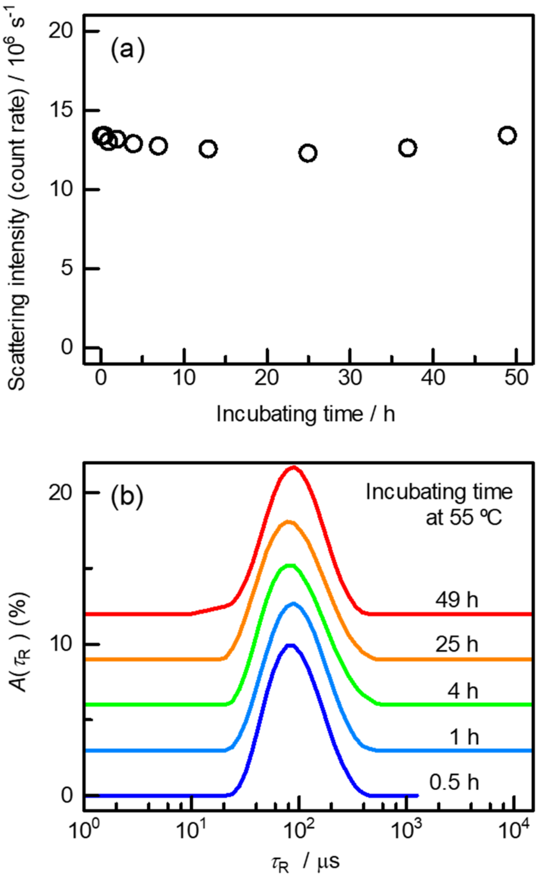

Figure 2-13. Temporal changes in (a) the scattering intensity of the 650 nm light and in (b) $A(\tau_R)$ of the 0.5 wt % aqueous solution of the PEO–PPO AMB copolymer $(EO_{220}PO_{33})_8$ at 55 °C.

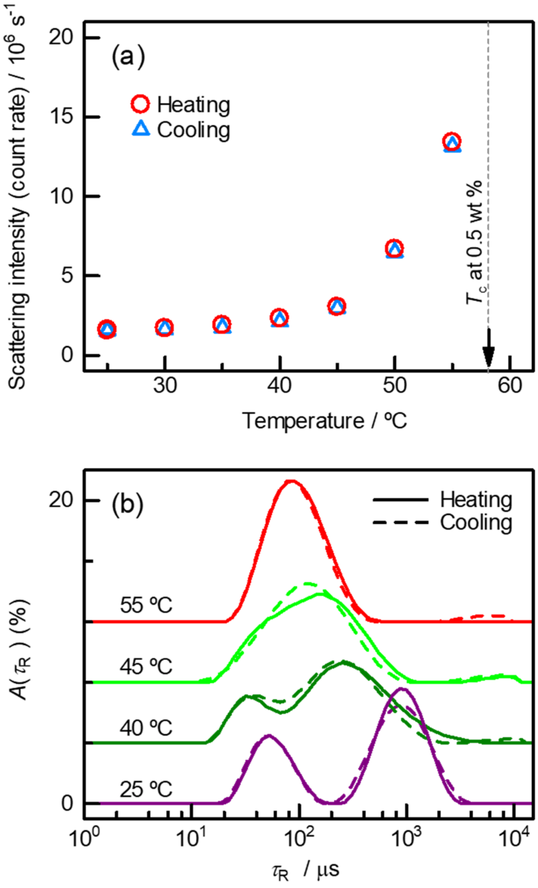

Figure 2-14. Temperature dependence of (a) the scattering intensity of the 650 nm light and (b) $A(\tau_R)$ of the 0.5 wt % aqueous solution of the PEO–PPO AMB copolymer $(EO_{220}PO_{33})_8$ monitored during the heating and cooling process.

causes an attractive force between hydrophobic groups in water, is based upon the entropy gain of the water molecules around the groups. The conventional picture has assumed a water "cage" around the hydrophobic groups[29], whereas more current studies have suggested that the gain of the translational entropy of water is the driving force of the hydrophobic interaction[30]. Both of them can rationalize that the hydrophobic interaction induces the micellization by heating under a positive enthalpic process. In this process, the entropy gain of water overwhelms the entropy loss because of the localization of the hydrophobic chains in the micelle core. It has been also known that the hydrophobic interaction often induces the LCST phase separation of the aqueous solution.

It is of interest whether the micellelike aggregate observed here is thermodynamically stable. First, we measured the temporal change in the scattering intensity and $A(\tau_R)$ for the 0.5 wt % aqueous solution of $(EO_{220}PO_{33})_8$ at 55 °C. As shown in Figure 2-13, the scattering intensity and $A(\tau_R)$ remain the same for at least 2 days. Second, the thermal history of the process is examined. Figure 2-14 represents the temperature dependence of the scattering intensity and $A(\tau_R)$ for the 0.5 wt % aqueous solution of $(EO_{220}PO_{33})_8$ during heating and cooling processes with the same rate. The solution is heated above T_c and then cooled down to 25 °C. As can be seen in the figure, no thermal hysteresis is observed for the scattering intensity, and the $A(\tau_R)$ at the same temperature is also in good agreement within a range of error. Thus, we have concluded that micellelike aggregates are formed under thermodynamically stable process.

2.3.3 Hydrophilicity of PEO–PPO AMB Copolymers

When the micellelike aggregate of the PEO–PPO AMB copolymers is formed in water upon heating, the interaction among the polymer chains should change from repulsive to attractive as the temperature increases. This can be evaluated from the second virial coefficient A_2 obtained through the SLS measurement. The Debye plot for the aqueous solution from the PEO–PPO AMB copolymers is shown in Figure 2-15a,b. In the case that the polymer concentration (c) is lower than 0.6 g L^{-1} (~0.06 wt %), the $Kc/\Delta R_\theta$ value shows a linear dependence on c. Above 0.8 g L^{-1}, the plot starts deviating from the linear correlation because the scattering intensity of the aggregates becomes significant. Note that at 0.05 wt %, the influence of the aggregate on the scattering intensity is small but not zero, as can be seen in Figure 2-12a.

Fitting of these data by eq. (1) gives rise to M_w and A_2 of the PEO–PPO AMB copolymer. Figure 2-15c,d show the M_w and A_2 values of $(EO_{220}PO_{33})_8$ and $(EO_{68}PO_{33})_9$, respectively. M_w of $(EO_{220}PO_{33})_8$ at 20–40 °C is ca. 1.3×10^5 g mol^{-1}, whereas that of $(EO_{68}PO_{33})_9$ at 15–30 °C is ca. 4.1×10^4 g mol^{-1}.

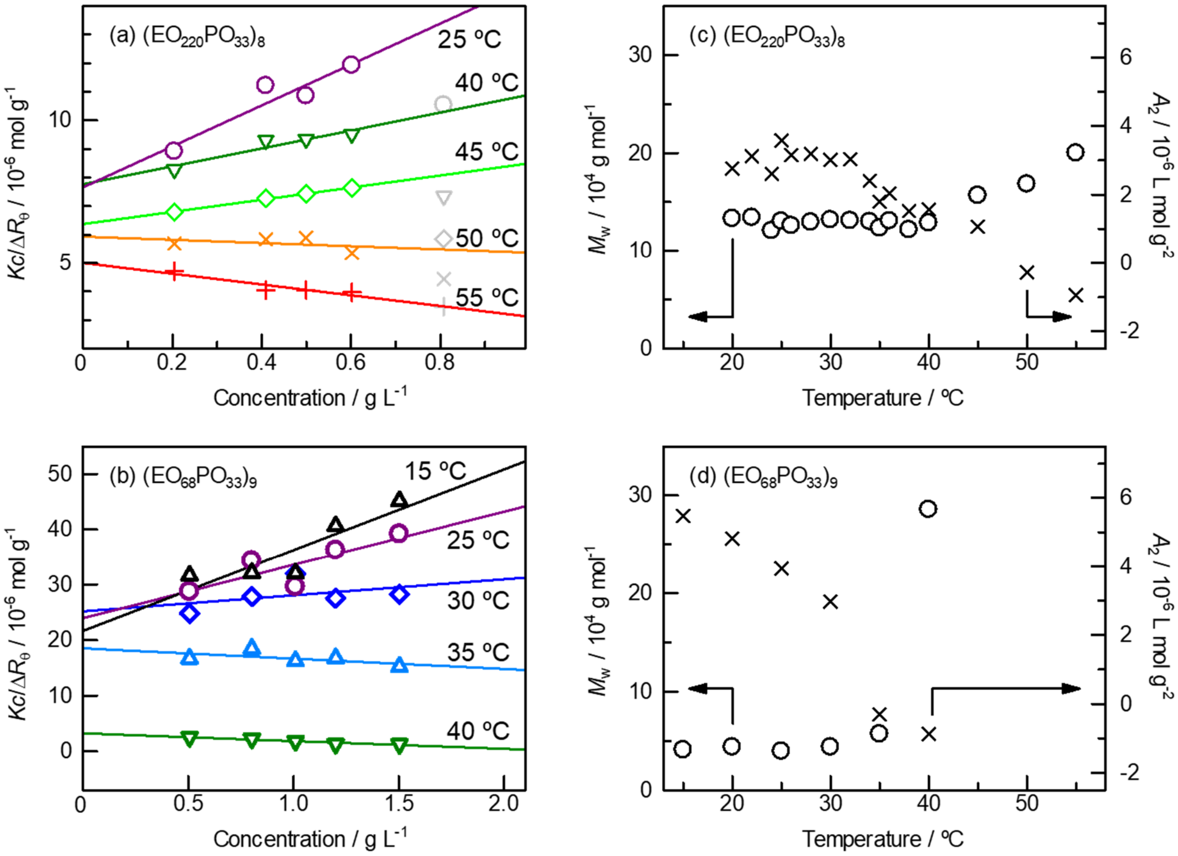

Figure 2-15. (a) Debye plot for the aqueous solutions of $(EO_{220}PO_{33})_8$ and (b) that for $(EO_{68}PO_{33})_9$ at 25 °C (circle), 40 °C (reverse triangle), 45 °C (diamond), 50 °C (diagonal cross), and 55 °C (cross). The solid lines show the fitting results by using Equation (1). Temperature dependence of M_w (circle) and A_2 (diagonal cross) estimated from the fitting results of the Debye plot; (c) $(EO_{220}PO_{33})_8$ and (d) $(EO_{68}PO_{33})_9$.

These values are similar to those estimated by SEC. As mentioned above, M_w and the number of PEO–PPO repeating pairs obtained from the Debye plot may be slightly overestimated because of the scattering from a tiny amount of aggregates. On the other hand, SEC overestimates M_w of PEO prepolymers but underestimates M_w of PPO prepolymers, as can be seen in Table 1.

The M_w value remains constant at a lower temperature. This suggests that the majority of the PEO–PPO AMB copolymers exist as a unimer in this temperature range. M_w of $(EO_{220}PO_{33})_8$ starts increasing above 40 °C, whereas that of $(EO_{68}PO_{33})_9$ rises up from 35 °C, indicating that the copolymer starts forming micellelike aggregates. On the other hand, the apparent A_2 values of $(EO_{220}PO_{33})_8$ and $(EO_{68}PO_{33})_9$ start going down before M_w increases. At a lower temperature, the PEO–PPO AMB copolymers are hydrophilic and water is a good solvent because a positive value of A_2 represents that the interaction between the copolymers is repulsive. The A_2 quantity of the PEO–PPO AMB copolymers at around 20 °C is smaller by 1 order of magnitude than that of poly(*N*-isopropylacrylamide) (PNiPAm) in water, which is the representative thermoresponsive polymer[31]. This means that the repulsive interaction between the PEO–PPO AMB copolymers is relatively weak.

The A_2 quantity of $(EO_{220}PO_{33})_8$ reaches 0 at around 50 °C, whereas that of $(EO_{68}PO_{33})_9$ reaches 0 at around 35 °C. These should be close to the T_θ of the PEO–PPO AMB copolymers in water. As a result of the decrement of A_2 (the increment of the attractive forces between the polymers), the micellelike aggregate may form. This scenario is consistent with the results of the DLS measurements. For the aqueous solution of PNiPAm, A_2 also decreases with elevating temperature, but the solution undergoes phase separation without the formation of micellelike aggregates[31].

It is interesting to compare the A_2 quantity of the aqueous solution of $(EO_{68}PO_{33})_9$ with that of Pluronic P85 $(EO_{25}PO_{40}EO_{25})$. Brown et al. have found that A_2 of Pluronic P85 in water decreases from ca. 2.5×10^{-6} to 0.1×10^{-6} L mol g^{-2} as the temperature increases[24]. A_2 of Pluronic P85 approaches 0 at around 40 °C, whereas for $(EO_{68}PO_{33})_9$, A_2 varies from 5.5×10^{-6} at 15 °C and becomes 0 near 35 °C. This implies that the intermolecular interaction among the Pluronic chains is similar to that among the PEO–PPO AMB copolymer chains, which may be associated with f_{PEO} of the copolymer. Alexandridis et al. have studied the thermodynamic quantities of micellization of 12 Pluronics in water including P85 and concluded that the PPO block of Pluronics is responsible for the micellization[11]. Because the temperature change in A_2 of $(\mathrm{EO}_{68}\mathrm{PO}_{33})_9$ is similar to that of P85, we inferred that the decrement in A_2 of the PEO–PPO AMB copolymers observed here is possibly induced by the hydrophobic interactions between the PPO blocks.

2.4 Conclusion

The PEO–PPO AMB copolymers having a different weight fraction of PEO, $(EO_{220}PO_{33})_8$ and $(EO_{68}PO_{33})_9$, are prepared by a dehydrated condensation reaction between α,ω-diamino PPO and α,ω-disuccinimidyl PEO prepolymers. The M_w values of $(EO_{220}PO_{33})_8$ and $(EO_{68}PO_{33})_9$ are estimated by SEC to be 1.7×10^5 and 5.7×10^4 g mol^{-1}, respectively. The SLS measurements support the results; the M_w values of $(EO_{220}PO_{33})_8$ and $(EO_{68}PO_{33})_9$ are 1.3×10^5 and 4.1×10^4 g mol^{-1}, respectively. The number of PEO–PPO repeating pairs in the PEO–PPO AMB copolymers obtained here is over 8.

The aqueous solution of the copolymer undergoes a phase separation with increasing temperature. For the aqueous solution of $(EO_{220}PO_{33})_8$, the phase boundary curve seems to have a shallow minimum at around 0.3 wt % and 58 °C, which should correspond to the LCST. On the other hand, the LCST for the aqueous solution of $(EO_{68}PO_{33})_9$ is estimated to be ca. 42 °C. The critical solution concentration for $(EO_{68}PO_{33})_9$ is not clear because the concentration dependence of T_c at a higher concentration range is very small. The DLS results suggest that $A(\tau_R)$ of the 0.5 wt % aqueous solution of the PEO–PPO AMB copolymers is bimodal at 25 °C, where the fast relaxation mode is assignable to the unimer with R_h = 5–10 nm. The temperature dependence of $A(\tau_R)$ suggests that a micellelike aggregate forms with increasing temperature. The R_h values of the aggregates are 20 nm for $(EO_{220}PO_{33})_8$ and 10 nm for $(EO_{68}PO_{33})_9$. This behavior is very similar to the micellization of Pluronics. The micellelike aggregate is thermally stable, and there is no thermal hysteresis in the formation of the aggregate.

The interaction between the PEO–PPO AMB copolymers in the aqueous solution is evaluated by using SLS measurements with the Debye plot. During the heating process, the apparent A_2 value of $(EO_{220}PO_{33})_8$ starts decreasing at 32 °C, and then M_w starts increasing above 40 °C. The T_θ of $(EO_{220}PO_{33})_8$ and $(EO_{68}PO_{33})_9$ in water are estimated to be around 50 and 35 °C, respectively. The increment of the attractive interaction between the PEO–PPO AMB copolymers results in the formation of the micellelike aggregates.

2.5 References

[1] Chiappetta, D. A.; Sosnik, A. Poly(ethylene Oxide)–poly(propylene Oxide) Block Copolymer Micelles as Drug Delivery Agents: Improved Hydrosolubility, Stability and Bioavailability of Drugs. *Eur. J. Pharm. Biopharm.* **2007**, *66* (3), 303–317.

[2] Gonzalez-Lopez, J.; Alvarez-Lorenzo, C.; Taboada, P.; Sosnik, A.; Sandez-Macho, I.; Concheiro, A. Self-Associative Behavior and Drug-Solubilizing Ability of Poloxamine (Tetronic) Block Copolymers. *Langmuir* **2008**, *24* (19), 10688–10697.

[3] Alexandridis, P.; Alan Hatton, T. Poly(ethylene Oxide)poly(propylene Oxide)poly(ethylene Oxide) Block Copolymer Surfactants in Aqueous Solutions and at Interfaces: Thermodynamics, Structure, Dynamics, and Modeling. *Colloids Surfaces A Physicochem. Eng. Asp.* **1995**, *96* (1–2), 1–46.

[4] Linse, P. Phase Behavior of Poly(ethylene Oxide)-Poly(propylene Oxide) Block Copolymers in Aqueous Solution. *J. Phys. Chem.* **1993**, *26* (17), 13896–13902.

[5] Schmolka, I. R. Artificial Skin I. Preparation and Properties of Pluronic F???127 Gels for Treatment of Burns. *J. Biomed. Mater. Res.* **1972**, *6* (6), 571–582.

[6] Nagarajan, R.; Ganesh, K. Block Copolymer Self-Assembly in Selective Solvents: Theory of Solubilization in Spherical Micelles. *Macromolecules* **1989**, *22* (11), 4312–4325.

[7] Nagarajan, R.; Barry, M.; Ruckenstein, E. Unusual Selectivity in Solubilization by Block Copolymer Micelles. *Langmuir* **1986**, *2* (2), 210–215.

[8] Nagarajan, R.; Ganesh, K. Comparison of Solubilization of Hydrocarbons in (PEO-PPO) Diblock versus (PEO-PPO-PEO) Triblock Copolymer Micelles. *J. Colloid Interface Sci.* **1996**, *184* (2), 489–499.

[9] Alexandridis, P.; Athanassiou, V.; Fukuda, S.; Hatton, T. A. Surface Activity of Poly(ethylene Oxide)-Block-Poly(propylene Oxide)-Block-Poly(ethylene Oxide) Copolymers. *Langmuir* **1994**, *10* (8), 2604–2612.

[10] Zhou, Z.; Chu, B. Light-Scattering Study on the Association Behavior of Triblock Polymers of Ethylene Oxide and Propylene Oxide in Aqueous Solution. *J. Colloid Interface Sci.* **1988**, *126* (1), 171–180.

[11] Alexandridis, P.; Holzwarth, J. F.; Hatton, T. A. Micellization of Poly(ethylene Oxide)-Poly(propylene Oxide)-Poly(ethylene Oxide) Triblock Copolymers in Aqueous Solutions: Thermodynamics of Copolymer Association. *Macromolecules* **1994**, *27* (9), 2414–2425.

[12] Sosnik, A.; Cohn, D. Reverse Thermo-Responsive Poly(ethylene Oxide) and Poly(propylene Oxide) Multiblock Copolymers. *Biomaterials* **2005**, *26* (4), 349–357.

[13] Sun, K. H.; Sohn, Y. S.; Jeong, B. Thermogelling Poly(ethylene Oxide-B-Propylene Oxide-B-Ethylene Oxide) Disulfide Multiblock Copolymer as a Thiol-Sensitive Degradable Polymer. *Biomacromolecules* **2006**, *7* (10), 2871–2877.

[14] Debye, P. Light Scattering in Solutions. *J. Appl. Phys.* **1944**, *15* (4), 338–342.

[15] Saeki, S.; Kuwahara, N.; Nakata, M.; Kaneko, M. Upper and Lower Critical Solution Temperatures in Poly (Ethylene Glycol) Solutions. *Polymer (Guildf).* **1976**, *17* (8), 685–689.

[16] Tasaki, K. Poly(oxyethylene)-Water Interactions: A Molecular Dynamics Study. *J. Am. Chem. Soc.* **1996**, *118* (35), 8459–8469.

[17] Shikata, T.; Okuzono, M.; Sugimoto, N. Temperature-Dependent Hydration/dehydration Behavior of Poly(ethylene Oxide)s in Aqueous Solution. *Macromolecules* **2013**, *46* (5), 1956–1961.

[18] Ataman, M. Properties of Aqueous Salt Solutions of Poly(ethylene Oxide). Cloud Points, θ Temperatures. *Colloid Polym. Sci.* **1987**, *265* (1), 19–25.

[19] Mitchard, N. M.; Beezer, a. E.; Mitchell, J. C.; Armstrong, J. K.; Chowdhry, B. Z.; Leharne, S.; Buckton, G. Thermodynamic Analysis of Scanning Calorimetric Transitions Observed for Dilute Aqueous Solutions of ABA Block Copolymers. *J. Phys. Chem.* **1992**, *96* (23), 9507–9512.

[20] Griffin, W. C. Classification of Surface-Active Agents by "HLB". *J. Soc. Cosmet. Chem.* **1949**, *1* (5), 311–326.

[21] Provencher, S. W. CONTIN: A General Purpose Constrained Regularization Program for Inverting Noisy Linear Algebraic and Integral Equations. *Comput. Phys. Commun.* **1982**, *27* (3), 229–242.

[22] Kanao, M.; Matsuda, Y.; Sato, T. Characterization of Polymer Solutions Containing a Small Amount of Aggregates by Static and Dynamic Light Scattering. *Macromolecules* **2003**, *36* (6), 2093–2102.

[23] Al-Saden, A. A.; Whateley, T. L.; Florence, A. T. Poloxamer Association in Aqueous Solution. *J. Colloid Interface Sci.* **1982**, *90* (2), 303–309.

[24] Brown, W.; Schillen, K.; Almgren, M.; Hvidt, S.; Bahadur, P. Micelle and Gel Formation in a Poly(ethylene Oxide)/poly(propylene Oxide)/poly(ethylene Oxide) Triblock Copolymer in Water Solution: Dynamic and Static Light Scattering and Oscillatory Shear Measurements. *J. Phys. Chem.* **1991**, *95* (4), 1850–1858.

[25] Lazzara, G.; Milioto, S.; Gradzielski, M. The Solubilisation Behaviour of Some Dichloroalkanes in Aqueous Solutions of PEO-PPO-PEO Triblock Copolymers: A Dynamic Light Scattering, Fluorescence Spectroscopy, and SANS Study. *Phys. Chem. Chem. Phys.* **2006**, *8* (19), 2299–2312.

[26] Hsu, Y. H.; Tsui, H. W.; Lee, C. F.; Chen, S. H.; Chen, L. J. Effect of Alcohols on the Heat of Micellization of Pluronic F88 Aqueous Solutions. *Colloid Polym. Sci.* **2015**, *293* (12), 3403–3415.

[27] Wanka, G.; Hoffmann, H.; Ulbricht, W. The Aggregation Behavior of Poly-(Oxyethylene)-Poly-(Oxypropylene)-Poly-(Oxyethylene)-Block-Copolymers in Aqueous Solution. *Colloid Polym. Sci.* **1990**, *268* (2), 101–117.

[28] Armstrong, J. K.; Parsonage, J.; Chowdhry, B.; Leharne, S.; Mitchell, J.; Beezer, A.; Loehner,

K.; Laggner, P. Scanning Densitometric and Calorimetric Studies of Poly(ethylene Oxide)/poly(propylene Oxide)/poly(ethylene Oxide) Triblock Copolymers (Poloxamers) in Dilute Aqueous Solution. *J. Phys. Chem.* **1993**, *97* (15), 3904–3909.

[29] Eisenberg, D.; Kauzmann, W. *The Structure and Properties of Water*; Clarendon Press, 2005.

[30] Harano, Y.; Kinoshita, M. Large Gain in Translational Entropy of Water Is a Major Driving Force in Protein Folding. *Chem. Phys. Lett.* **2004**, *399* (4–6), 342–348.

[31] Oribe, M.; Sato, T. Repulsive and Attractive Interactions between Polystyrene Chains in a Poor Solvent. *Polym. J.* **2004**, *36* (9), 747–753.

[32] Kubota, K.; Fujishige, S.; Ando, I. Solution Properties of poly(N-Isopropylacrylamide) in Water. *Polym. J.* **1990**, *22* (1), 15–20.

CHAPTER 3

Effect of Molecular Weight on Phase Separation of Polymer Solution

3.1 Introduction

Thermoresponsive polymers are a class of smart materials. The properties of such polymers change significantly in a controlled fashion under the influence of external stimuli[1]. To develop synthetic polymer systems that act as protein mimics is a great challenge for polymer scientists. The block design of copolymers is an effective strategy for preparing protein mimics using synthetic polymers[2]. An alternative way is to control the monomer sequence, which corresponds to the primary structure of proteins[3]. However, the interaction among the monomers often makes it difficult to predict the macroscopic properties of the final products[4,5]. In comparison with monomer sequence control, the block design is advantageous for achieving predictable physicochemical properties of the resultant copolymer and scale-up of the preparation process. Because the individual blocks in the copolymer may retain the characteristics of the homopolymer, the numerous reports on the homopolymers may serve as a block library[6–19].

Recently, we investigated the solution properties of amphiphilic alternating multiblock (AMB) copolymers. The AMB copolymer of poly(ethylene oxide) (PEO) and poly(propylene oxide) (PPO), i.e., the PEO–PPO AMB copolymer, exhibits amphiphilic features comparable to those of Pluronic and Ploxamer. Unique characteristics of the AMB configuration were observed for the unimer morphology in water. Previously, we found that the unimer of PEO–PPO AMB copolymers in water forms a core–corona structure similar to flower micelles[20]. This may arise from two factors: the hydrophobic interaction among the PPO blocks in the core and the repulsion among the unimers based upon stabilization of the PEO chain at the corona. When the hydrophilic interaction was not sufficiently strong, the unimer of the AMB copolymers could not form a core–corona structure. Indeed, the AMB copolymer of PEO and poly(*N*-ipropylacrylamide) (PNiPAm) adopts a random-coil conformation in water at room temperature, because PNiPAm tends to be well hydrated compared with PPO[2]. Because the PPO blocks are sufficiently hydrophobic to form a unimer micelle, the PEO–PPO

AMB copolymer can also be expected to serve as a simple model of multipass transmembrane proteins such as bacteriorhodopsin[21].

Although the PEO–PPO AMB copolymers possess interesting features as above mentioned, the fundamental aspects have yet to be fully revealed. In this study, we focus on the effect of the molecular weight on the cloud point (T_c) of the copolymers. Based on the literature concerning PEO–PPO–PEO triblock copolymers[22], the hydrophobicity of PEO–PPO block copolymers is essentially proportional to the molecular weight of PEO and PPO when the weight fraction of PEO (f_{PEO}) is constant. For the AMB copolymers, however, the molecular weight of the PEO and PPO blocks is fixed, but the number of PEO–PPO repeating pairs varies depending on the total molecular weight. Herein, PEO–PPO AMB copolymers with various molecular weights are prepared by precipitation fractionation. The fractionated samples are used to investigate the T_c of the aqueous solution.

3.2 Experimental Section

3.2.1 Preparation of PEO–PPO AMB copolymer

The PEO–PPO AMB copolymer was prepared by a dehydrated condensation reaction according to the literature[23]. Briefly, α,ω-diamino PPO (JEFFAMINE D-2000; weight-average molecular weight (M_w) = 2,000) was kindly supplied by Huntsman Corporation. α,ω-Disuccinimidyl PEO (SUNBRIGHT DE-100HS; M_w = 10,000) was purchased from NOF Corporation. The reaction was carried out in chloroform solution at 0 °C. The crude sample was recovered by dialysis against water, followed by freeze-drying. Precipitation fractionation of the copolymer was performed by phase separation in an acetone/*n*-hexane mixture at 25–50 °C. The PEO–PPO AMB copolymer prepared herein is denoted as $(EO_{220}PO_{33})_n$, where EO is the ethylene oxide unit, PO is the propylene oxide unit, and *n* is the number of PEO–PPO repeating units. The characterization details can be found in previous reports[20,23].

3.2.2 Size Exclusion Chromatography

The Size exclusion chromatography (SEC) apparatus consisted of a Jasco Intelligent HPLC system equipped with a guard column (SB-G, Shodex), two separation columns (SB-802.5HQ and SB-806MHQ, Shodex), and a refractive index detector (RI-2031Plus, Jasco). *N,N*-Dimethylformamide (HPLC grade, Wako) with 10 mM LiBr was used as the eluent at a flow rate of 0.35 mL min^{-1}, at 60 °C. The number-average molecular weight (M_n), M_w, and the polydispersity (M_w/M_n) were evaluated with respect to standard polystyrene samples with ten different peak-top molecular weights in the range of 1.22×10^3 to 2.70×10^6 (STANDARD SM-105, Shodex).

3.2.3 ^{1}H NMR and IR Spectroscopies

The ratio of EO units to PO units (*EO/PO*) in the PEO–PPO AMB copolymers was determined from the ^{1}H NMR spectra recorded on an Ascend 400 (Bruker) instrument at 400 MHz. All spectra were acquired at 25 °C using 1.0 wt% D_2O solutions.

3.2.4 Turbidity Measurements

The transmittance of 633 nm light through the polymer solution was monitored by using a UV–Vis spectrophotometer (V-630iRM, Jasco) equipped with a temperature controller (ETCS-761, Jasco). The sample was heated at a rate of 1.0 °C min^{-1}. The cloud point (T_c) was defined by referring to the first derivative of the transmittance curve.

3.3 Results and Discussion

3.3.1 Characterization of Fractionated Samples

Figure 3-1 shows the SEC charts of the PEO–PPO AMB copolymers, $(EO_{220}PO_{33})_n$, before and after precipitation fractionation. Two peaks at 2270 and 2330 s were apparent in the SEC chart of the last fraction. Thus, we did not analyze this sample (denoted as “residue” in Figure 3-1). The SEC charts of fraction 1–3 showed a systematic shift, indicating differences in the M_n of each fraction. The estimated M_n and M_w/M_n values are listed in Table 2. Although fractionation appeared to be successful based on the M_n of each fraction, the M_w/M_n values were still large (1.7–2.4). In general, fractionation of copolymers is more difficult than fractionation of homopolymers because the solubility of copolymers is also influenced by their chemical composition[24]. To estimate *EO/PO* for the fractionated samples, the ^1H NMR spectra were acquired (Figure 3-2). The peak at $\delta = 3.7$ ppm arises from the methylene proton of the EO and PO units, while the peak at $\delta = 1.2$ ppm is due to the methyl proton of the PO unit. The *EO/PO* of the copolymers was estimated to be 6.7–6.9. Because the PEO block contains 220 EO units and the PPO block has 33 PO units, the one-by-one connection of PEO

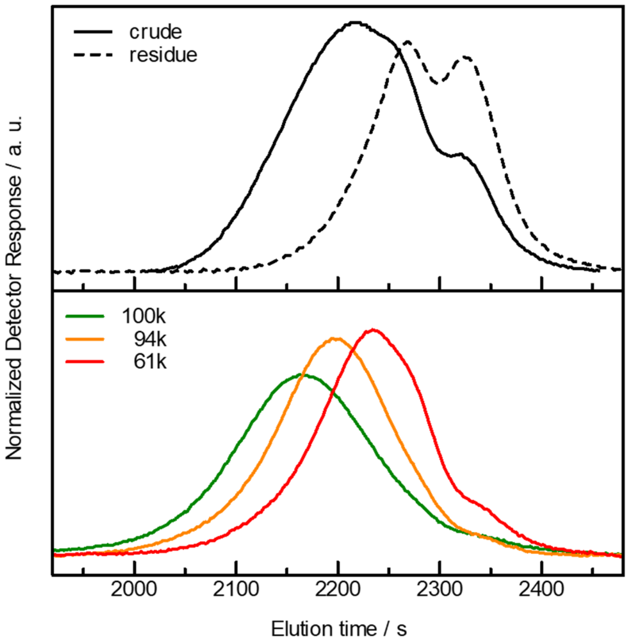

Figure 3-1. SEC charts of the crude and each fractions of the PEO–PPO AMB copolymer.

and PPO yields *EO/PO* = 6.7. Thus, we can assume that the PEO–PPO AMB copolymers contain an equal amount of PEO and PPO blocks and the chemical composition of each fractionated sample is similar.

The SEC and ^{1}H NMR results indicate successful precipitation fractionation of the PEO–PPO AMB copolymer. The *n* value for $(EO_{220}PO_{33})_n$ was estimated to range from 3.3 to 5.4. When *n*-hexane as a poor solvent was added to the acetone solution, the PEO–PPO AMB copolymers precipitated in

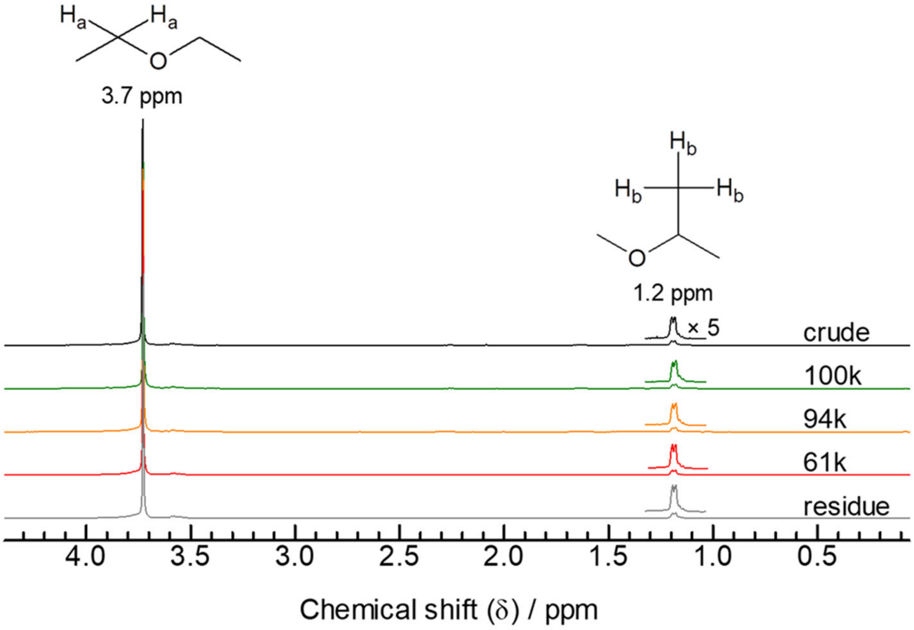

Figure 3-2. ^{1}H NMR spectra of the fractionated PEO–PPO AMB copolymers, the crude, and the residue.

Table 2. Molecular weight (M_n), polydispersity (M_w/M_n), the ratio of EO units to PO units (*EO/PO*), and the number of repeating units (*n*) of PEO–PPO AMB copolymers.

sample	fraction	M_n (M_w/M_n) [a]	*EO/PO*[b]	*n*
crude	—	7.2×10^4 (3.3)	—	—
120k[c]	—	1.2×10^5 (1.5)	6.6	6.3
100k	1	1.0×10^5 (2.4)	6.9	5.4
94k	2	9.4×10^4 (1.7)	6.7	5.1
61k	3	6.1×10^4 (1.8)	6.9	3.3

[a] Size exclusion chromatography with polystyrene standards. [b] Estimated by intensity of the peak at 3.7 ppm and 1.2 ppm obtained from ^{1}H NMR. [c] The fraction was obtained from a different lot.

the order of the molecular weight. Interestingly, this behavior is similar to the precipitation fractionation of homopolymers. Thus, we presumed that the *EO/PO* for a single chain did not differ in the PEO–PPO AMB copolymers prepared by amide condensation.

3.3.2 Molecular Weight Dependence of T_c for PEO–PPO AMB Copolymer in Water

The results of the turbidity measurement for the copolymers are shown in Figure 3-3. The T_c values were clearly high for the crude sample and the residue. As shown in Figure 3-1, the residue contained a certain amount of impurity, corresponding to the peak at 2320 s in the SEC chart. The T_c of the crude sample may also contain a large contribution from the impurity. Thus, we assumed that there is a short PEO–PPO block copolymer in the crude sample and the residue, resulting in the high T_c. Note that the aqueous solution of the PEO homopolymer with $M_n = 14{,}000$ g mol^{-1} undergoes phase separation around 107 °C[25], whereas the T_c of an aqueous solution of Pluronic F88, for which the *EO/PO* ratio is similar to that of $(EO_{220}PO_{33})_n$ synthesized herein, is over 100 °C[26].

Figure 3-4 shows the molecular weight dependence of T_c for the aqueous solution of the PEO–PPO AMB copolymers. The T_c decreased with increasing M_n, which is typical for polymer solutions

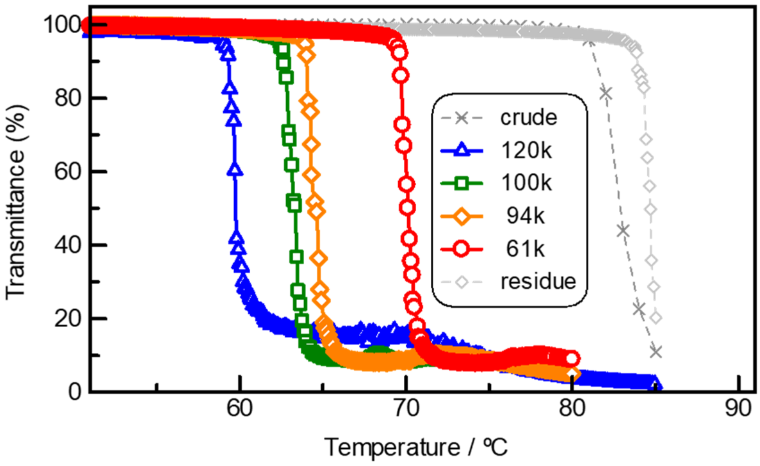

Figure 3-3. Temperature dependence of the transmittance of the 633 nm light passing through the aqueous solution of the PEO–PPO AMB copolymers. The polymer concentration is 1.5 wt % except for the 120k fraction (1.0 wt %).

that undergo phase separation with a lower critical solution temperature (LCST), such as the PEO/water[25] and poly(*N,N*-diethylacryladmide)/water[27] systems. On the other hand, poly(*N*-isopropylacrylamide)/water system, which is a quite popular system that undergoes LCST-type phase separation, shows an abnormal M_n dependence on T_c, in which T_c decreases with decreasing M_n[28].

The inset of Figure 3-4 shows the plot of $1/T_\mathrm{c}$ against $1/N^{0.5} + 1/2N$, where N is the number of monomer units (both of EO and PO) in the AMB copolymer. According to the Shultz–Flory theory[29], the critical solution temperature (T_cp) of a polymer solution is correlated with the polymerization degree as:

$$\frac{T_\theta}{T_\mathrm{cp}} = 1 + \frac{1}{\psi}\left(\frac{1}{\sqrt{N}} - \frac{1}{2N}\right) \tag{2}$$

where T_θ is Flory's theta temperature and ψ is the entropy parameter[30]. Clearly, T_cp is not equal to the T_c measured herein. In a previous paper, however, we reported that the T_c of the aqueous solution of PEO–PPO AMB copolymers is insensitive to the polymer concentration above T_cp, which is located

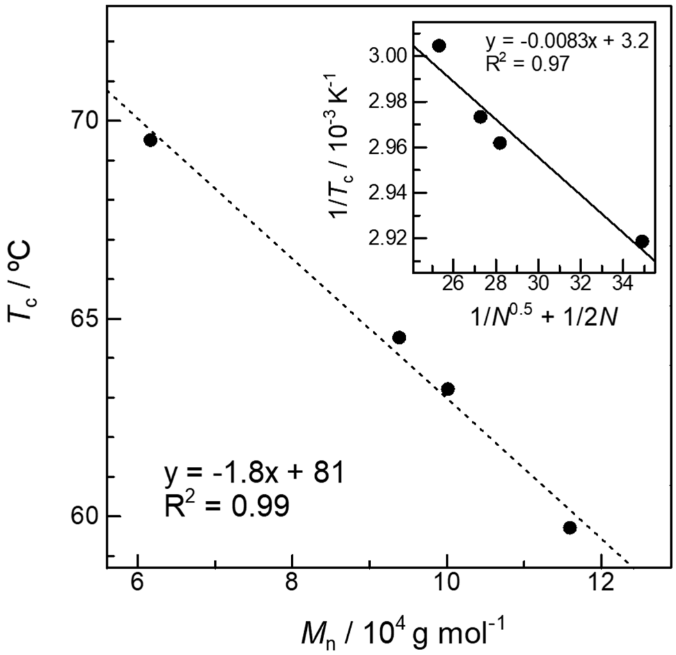

Figure 3-4. Concentration dependence of the cloud point (T_c) for the aqueous solutions of each PEO–PPO AMB copolymer. The T_c is determined by the transmittance curve measured with light at 633 nm.

at ca. 0.3 wt%[23]. Thus, the T_c measured for the 1.5 wt % aqueous solution of the copolymers is expected to be close to the T_{cp}. The intercept of the solid line in the inset gives a value of 39 °C, which corresponds to the T_θ of the system. In previous papers, we reported that the micellization temperature of $(EO_{220}PO_{33})_6$ is around 41–50 °C[20] and the second virial coefficient, A_2, of $(EO_{220}PO_{33})_8$ approaches zero around 50 °C[23]. The results shown here imply that the Shultz–Flory theory is applicable even to PEO–PPO AMB copolymers.

3.4 Conclusion

We investigated the effect of the molecular weight on the T_c of aqueous solutions of PEO–PPO AMB copolymers with various molecular weights. The PEO–PPO AMB copolymers were obtained by precipitation fractionation. The T_c of the aqueous solution of the PEO–PPO AMB copolymer decreases as the M_n increases. The results imply that the Shultz–Flory theory is applicable to the PEO–PPO AMB copolymer/water system.

3.5 References

[1] Kobayashi, J.; Okano, T. Design of Temperature-Responsive Polymer-Grafted Surfaces for Cell Sheet Preparation and Manipulation. *Bull. Chem. Soc. Jpn.* **2019**, *92*, 817–824.

[2] Rikiyama, K.;Sanada, Y.; Watanabe, K.; Aida, M.; Katsumoto, Y. Unimer Structure and Micellization of Poly(ethylene oxide)-Stereocontrolled Poly(*N*-isopropylacrylamide) Alternating Multiblock Copolymers in Aqueous Solution. *Macromolecules*. **2019**, *52*, 7188-7196.

[3] Lutz, J. F. A controlled sequence of events. *Nat. Chem.* **2010**, *2*, 84–85.

[4] Keerl, M.; Richtering, W. Synergistic depression of volume phase transition temperature in copolymer microgels. *Colloid Polym. Sci.* **2007**, *285*, 471–474.

[5] Maeda, Y.; Yamabe, M. A unique phase behavior of random copolymer of N-isopropylacrylamide and N,N-diethylacrylamide in water. *Polymer (Guildf).* **2009**, *50*, 519–523.

[6] Engelis, N. G.; Anastasaki, A.; Nurumbetov, G.; Truong, N. P.; Nikolaou, V.; Shegiwal, A.; Whittaker, M. R.; Davis, T. P.; Haddleton, D. M. Sequence-controlled methacrylic multiblock copolymers via sulfur-free RAFT emulsion polymerization. *Nat. Chem.* **2017**, *9*, 171–178.

[7] Gody, G.; Barbey, R.; Danial, M.; Perrier, S. Ultrafast RAFT polymerization: Multiblock copolymers within minutes. *Polym. Chem.* **2015**, *6*, 1502–1511.

[8] Gody, G.; Maschmeyer, T.; Zetterlund, P. B.; Perrier, S. Rapid and quantitative one-pot synthesis of sequence-controlled polymers by radical polymerization. *Nat. Commun.* **2013**, *4*, 1–9.

[9] Simula, A.; Nikolaou, V.; Anastasaki, A.; Alsubaie, F.; Nurumbetov, G.; Wilson, P.; Kempe, K.; Haddleton, D. M. Synthesis of well-defined α,ω-telechelic multiblock copolymers in aqueous medium: In situ generation of α,ω-diols. *Polym. Chem.* **2015**, *6*, 2226–2233.

[10] Anastasaki, A.; Oschmann, B.; Willenbacher, J.; Melker, A.; Van Son, M. H. C.; Truong, N. P.; Schulze, M. W.; Discekici, E. H.; McGrath, A. J.; Davis, T. P.; Bates, C. M.; Hawker, C. J. One-Pot Synthesis of ABCDE Multiblock Copolymers with Hydrophobic, Hydrophilic, and Semi-Fluorinated Segments. *Angew. Chemie - Int. Ed.* **2017**, *56*, 14483–14487.

[11] Carroll, D. R.; Constantinou, A. P.; Stingelin, N.; Georgiou, T. K. Scalable syntheses of well-defined pentadecablock bipolymer and quintopolymer. *Polym. Chem.* **2018**, *9*, 3450–3454.

[12] Zhang, Q.; Anastasaki, A.; Li, G. Z.; Haddleton, A. J.; Wilson, P.; Haddleton, D. M. Sequence-controlled multi-block glycopolymers to inhibit DC-SIGN-gp120 binding. *Angew. Chemie - Int. Ed.* **2013,** *52*, 4435–4439.

[13] Alsubaie, F.; Anastasaki, A.; Wilson, P.; Haddleton, D. M. Sequence-controlled multi-block copolymerization of acrylamides via aqueous SET-LRP at 0 °c. *Polym. Chem.* **2015**, *6*, 406–417.

[14] Zhang, Q.; Collins, J.; Anastasaki, A.; Wallis, R.; Mitchell, D. A.; Becer, C. R.; Haddleton, D. M. Multiblock sequence-controlled glycopolymers via Cu(0)-LRP following efficient thiol-halogen, thiol-epoxy and CuAAC reactions. *Polym. Chem.* **2014**, *5*, 3876–3883.

[15] Determan, M. D.; Cox, J. P.; Seifert, S.; Thiyagarajan, P.; Mallapragada, S. K. Synthesis and

characterization of temperature and pH-responsive pentablock copolymers. *Polymer (Guildf).* **2005**, *46*, 6933–6946.

[16] Determan, M. D.; Guo, L.; Thiyagarajan, P.; Mallapragada, S. K. Supramolecular self-assembly of multiblock copolymers in aqueous solution. *Langmuir* **2006**, *22*, 1469–1473.

[17] Peleshanko, S.; Anderson, K. D.; Goodman, M.; Determan, M. D.; Mallapragada, S. K.; Tsukruk, V. V. Thermoresponsive reversible behavior of multistimuli pluronic-based pentablock copolymer at the air-water interface. *Langmuir* **2007**, *23*, 25–30.

[18] Lu, Y.; Chen, T.; Mei, A.; Chen, T.; Ding, Y.; Zhang, X.; Xu, J.; Fan, Z.; Du, B. Solution behaviors and microstructures of PNIPAm-P123-PNIPAm pentablock terpolymers in dilute and concentrated aqueous solutions. *Phys. Chem. Chem. Phys.* **2013**, *15*, 8276–8286.

[19] Zhou, Y.; Jiang, K.; Song, Q.; Liu, S. Thermo-induced formation of unimolecular and multimolecular micelles from novel double hydrophilic multiblock copolymers of N,N-dimethylacrylamide and N-isopropylacrylamide. *Langmuir* **2007**, *23*, 13076–13084.

[20] Rikiyama, K.; Horiuchi, T.; Koga, N.; Sanada, Y.; Watanabe, K.; Aida, M.; Katsumoto, Y. Micellization of poly(ethylene oxide)-poly(propylene oxide) alternating multiblock copolymers in water. *Polymer (Guildf).* **2018**, *156*, 102–110.

[21] Muraoka, T.; Shima, T.; Hamada, T.; Morita, M.; Takagi, M.; Kinbara, K. Mimicking multipass transmembrane proteins: Synthesis, assembly and folding of alternating amphiphilic multiblock molecules in liposomal membranes. *Chem. Commun.* **2011**, *47*, 194–196.

[22] Alexandridis, P.; Holzwarth, J. F.; Hatton, T. A. Micellization of Poly(ethylene oxide)-Poly(propylene oxide)-Poly(ethylene oxide) Triblock Copolymers in Aqueous Solutions: Thermodynamics of Copolymer Association. *Macromolecules* **1994**, *27*, 2414–2425.

[23] Horiuchi, T.; Sakai, T.; Sanada, Y.; Watanabe, K.; Aida, M.; Katsumoto, Y. Association Behavior of Poly(ethylene oxide)-Poly(propylene oxide) alternating multiblock copolymers in water toward thermally induced phase separation. *Langmuir* **2017**, *33*, 14649–14656.

[24] Francuskiewicz, F. *Polymer Fractionation*. Springer, Berlin (1994).

[25] Saeki, S.; Kuwahara, N.; Nakata, M.; Kaneko, M. Upper and lower critical solution temperatures in poly (ethylene glycol) solutions. *Polymer (Guildf).* **1976**, *17*, 685–689.

[26] Alexandridis, P.; Alan Hatton, T. Poly(ethylene oxide)poly(propylene oxide)poly(ethylene oxide) block copolymer surfactants in aqueous solutions and at interfaces: thermodynamics, structure, dynamics, and modeling. *Colloids Surfaces A Physicochem. Eng. Asp.* **1995**, *96*, 1–46.

[27] Watanabe, R.; Takaseki, K.; Katsumata, M.; Matsushita, D.; Ida, D.; Osa, M. Characterization of poly(N,N-diethylacrylamide) and cloud points in its aqueous solutions. *Polym. J.* **2016**, *48*, 621–628.

[28] Tong, Z.; Zeng, F.; Zheng, X.; Sato, T. Inverse molecular weight dependence of cloud points for aqueous poly(N-isopropylacrylamide) solutions. *Macromolecules* **1999**, *32*, 4488–4490.

[29] Shultz, A. R.; Flory, P. J. Phase Equilibria in Polymer–Solvent Systems. *J. Am. Chem. Soc.* **1952**, *74*, 4760–4767.

[30] Hamada, F.; Fujisawa, K.; Nakajima, A. Lower Critical Solution Temperature in Linear Polyethylene–n-Alkane Systems. *Polym. J.* **1973**, *4*, 316–322.

CHAPTER 4

General Conclusion

We investigated the properties of the aqueous solution of PEO–PPO AMB copolymer with various molecular weight and different weight fraction of PEO.

The PEO–PPO AMB copolymers having a different weight fraction of PEO were prepared by a dehydrated condensation reaction between α,ω-diamino PPO and α,ω-disuccinimidyl PEO prepolymers. The copolymers with various molecular weights were obtained by precipitation fractionation. The aqueous solution of the copolymer underwent a LCST-type phase separation with increasing temperature. The T_c of the aqueous solution of the copolymer decreased as the weight fraction of PPO and the M_n of copolymer increased. These results suggest following:

(1) T_c of the aqueous solution of the PEO–PPO AMB copolymer is lower than that of PEO–PPO–PEO triblock copolymer having similar PEO weight fraction. The result is caused by the M_w of the PEO–PPO AMB copolymer which is much larger than that of the triblock copolymer.

(2) The hydrophobicity of the PEO–PPO AMB copolymer is correlated with the weight fraction of PEO like as that of triblock copolymers.

(3) Shultz–Flory theory, which is proposed for homopolymer systems, is possibly applicable to the AMB copolymer system.

These finding imply that the block design of the AMB copolymer has a potential to apply for designing functional materials such as protein mimics.

公表論文

(1) Horiuchi, Tasuku; Sakai, Takamasa; Sanada, Yusuke; Watanabe, Keisuke; Aida, Misako; Katsumoto, Yukiteru
Association Behavior of Poly(ethylene oxide)–Poly(propylene oxide) Alternating Multiblock Copolymers in Water toward Thermally Induced Phase Separation.
Langmuir **2017**, *33*, 14649–14656.

(2) Horiuchi, Tasuku; Rikiyama, Kazuaki; Sakanaya, Kenji; Sanada, Yusuke; Watanabe, Keisuke; Aida, Misako; Katsumoto, Yukiteru
Effect of Molecular Weight on Cloud Point of Aqueous Solution of Poly(ethylene oxide)–Poly(propylene oxide) Alternating Multiblock Copolymer.
J. Oleo Sci. (in press)

参考論文

(1) Rikiyama, Kazuaki; Horiuchi, Tasuku; Koga, Naoyuki; Sanada, Yusuke; Watanabe, Keisuke; Aida, Misako; Katsumoto, Yukiteru
Micellization of Poly(Ethylene Oxide)–Poly(Propylene Oxide) Alternating Multiblock Copolymers in Water.
Polymer **2018**, *156*, 102–110.